The Sixteenth International Congress on Sound and Vibration
Kraków, 5-9 July 2009

PREDICTION OF LOCK-IN RANGE BY SPECTRAL ANALYSIS, AND ANALYTICAL VERIFICATION OF THE GRIFFIN PLOT

Anoshiravan Farshidianfar, Hossein Zanganeh

Department of mechanical engineering, Ferdowsi University of Mashhad, Mashhad, Iran
e-mail: farshid@um.ac.ir

Vortex-induced vibrations (VIV) are a well-known phenomenon to engineers. The practical significance of VIV has led to a large number of fundamental studies. In this paper, the behavior of an elastically mounted cylinder, subjected to (VIV), is investigated by a wake oscillator model. First the spectral analysis of the model is used as a criterion for the predicting of the lock-in range, in both low and high mass-damping ratios. Then the validity of using a combined mass-damping parameter for predicting of the maximum structure displacement amplitude at lock-in, is analytically investigated.

1. Introduction

The VIV phenomenon is result of the interaction between fluid and structure. In explanation of its occurance procedure it can be said that, a cross-flow blowing over bluff bodies is usually unsteady. Beyond a critical Reynolds number, the boundary layer will separate from each side of the body to form the so-called Kármán vortex street. The alternately shed vortices from the body generate periodic forces on the structure, causing a structural vibration. The structural motion in turn influences the flow field, giving rise to nonlinear fluid–structure interaction[1].

The fluid structure interaction (coupling of fluctuating lift force and vibrating structure) can be modeled by the simple concept of a wake oscillator. In such models the wake dynamics follow a van der Pol equation. In fact it is sufficient to have a self sustained oscillator with a limit cycle. The bluff body is then considered as another oscillator excited by the wake variable[2]. Conversely the effect of the solid motion on the wake is represented by a forcing on the van der Pol equation that can be proportional to displacement, velocity or acceleration of bluff body. Facchinetti *et al.*[3] have shown that the most appropriate forcing is proportional to the acceleration of the bluff body.

In the dynamics of coupled fluid-structure systems, the phenomenon of frequency lock-in is often referred to. The lock-in range and the maximum structure displacement amplitude at lock-in, are two important topics of this field. The later is expressed as a function of a single combined mass-damping parameter, namely the Skop-Griffin parameter S_G, yielding the so-called Griffin plot[4]. The validity of the Griffin plot is one of important questions that have been debated over last three decades[5]. The main aims of this paper, using a wake oscillator model, are to find the lock-in range and to analytically verify the Griffin plot.

2. VIV model

The structure is an elastically mounted cylinder of diameter D. It is subjected to fluid flow of steady velocity U and can oscillate transversely to fluid flow, Fig. 1. The motion of this cylinder can be modelled by a simple linear equation that is affected by fluid loading, Eq. (1),

$$(m_s + m_f)\ddot{Y} + (c_s + c_f)\dot{Y} + kY = S \tag{1}$$

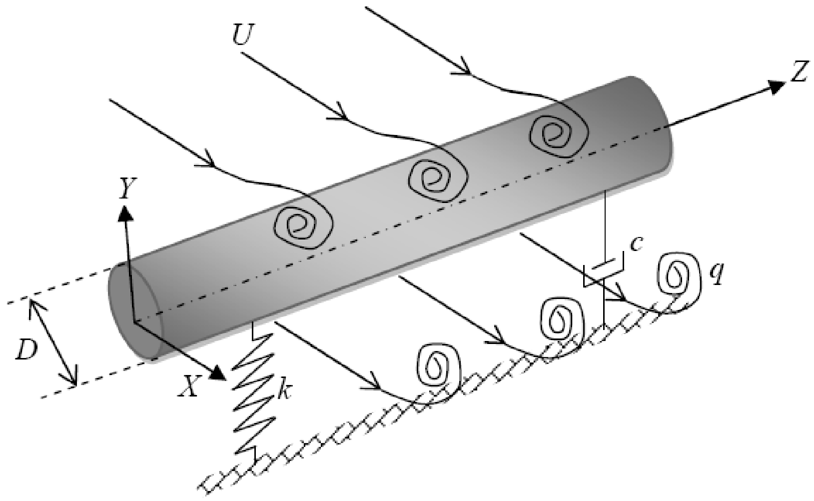

Figure 1. Model of elastically mounted cylinder coupled with wake oscillators for 2-D vortex-induced vibrations.

where overdots means derivatives with respect to dimensional time T and Y is the in-plane displacement of cylinder, transversely to fluid flow. m_s and k are, respectively, the mass and the stiffness of the cylinder in absence of fluid. c_s models viscous dissipations in supports. m_f is fluid-added mass which models invisid inertia effects of fluid[1] and c_f is the fluid-added damping. The forcing term S models the effects of vortices on structure and reads,

$$\begin{cases} m_f = \frac{1}{4}\pi C_m \rho D^2 \\ c_f = \frac{2\pi \mathrm{S_t} U}{D}\gamma\rho D^2 \\ S = \frac{1}{2}\rho U^2 D C_L \end{cases} \tag{2}$$

where ρ is the fluid density, C_m is the added mass coefficient that for a circular cylinder it reads $C_m=1$ [1], $\mathrm{S_t}$ is the Strouhal number and γ is the fluid added damping coefficient depending on the mean sectional drag coefficient C_D [1] and we assume that[3] $\gamma=0.8$. C_L is the fluctuating lift coefficient.

The fluctuating nature of the vortex street can be modelled by a van der Pol oscillator[6]

$$\ddot{q} + \varepsilon\Omega_f(q^2 - 1)\dot{q} + \Omega_f^2 q = \frac{A}{D}\ddot{Y} \tag{3}$$

where $\Omega_f=2\pi U\mathrm{S_t}/D$ is the vortex-shedding frequency, ε and A are the parameters that can be derived from experimental results, such as $\varepsilon=0.3$ and $A=12$ [3]. q is the dimensionless wake variable and is defined as $q(t)=2C_L(t)/C_{L0}$, where C_{L0} is the reference lift coefficient of a stationary cylinder subjected to vortex shedding that is usually taken as $C_{L0}=0.3$[1].

Eqs. (1) and (3) lead to the coupled fluid-structure dynamical system. There are different coupling methods, such as displacement coupling, velocity coupling and acceleration coupling. Facchinetti *et al*[3]. have shown that the most appropriate coupling is the acceleration coupling. So in the present paper, an acceleration coupling is used.

The Eqs. (1) and (3) can be put in a dimensionless form by introducing the dimensionless terms of $t = \sqrt{\frac{k}{m}}T$ and $y=Y/D$ that reads,

$$\begin{cases} \ddot{y} + \lambda\dot{y} + y = M\Omega^2 q \\ \ddot{q} + \varepsilon\Omega(q^2-1)\dot{q} + \Omega^2 q = A\ddot{y} \end{cases} \tag{4}$$

where $\Omega=\Omega_f/\Omega_s= S_t U_r$ is the dimensionless frequency of a self-sustained oscillation of the wake[2], $U_r=U/f_v D$ is the reduced velocity and f_v is the vortex-shedding frequency. λ is the damping coefficient and M is a mass number which scales the effects of the wake on the structure[3]. They read,

$$\begin{cases} \lambda = 2\xi + \frac{\gamma}{\mu}\Omega \\ M = \frac{\frac{c_{L0}}{2}}{8\pi^2 S_t^2 \mu} \\ \mu = \frac{m_s+m_f}{\rho D^2} \end{cases} \tag{5}$$

where ξ is the structure reduced damping, $\xi = \frac{c_s}{2\sqrt{km}}$

3. Prediction of lock-in domain

During lock-in phenomenon, the frequency of vortex shedding and the frequency of the structural oscillations synchronize and lock_into each other. Therefore, as it is expected and demonstrated by the experimental results, for the self-excited vibrations in the lock-in region, nearly harmonic oscillations will occur[7]. The spectral analysis is used as a criterion for identifying the harmonic and periodic behavior of a system. For harmonic motion, the spectrum has peaks of a fundamental and its harmonics. The deviation of the system from this behavior gives broad band components to the spectrum. In this section, using spectral analysis, the lock-in domain at both low and high mass damping ratios is predicted.

The experimental results of Feng[8] and Branković and Bearman[9], that were conducted at high and low mass-damping ratios, respectively, are shown in Fig. 2. As seen, the behavior of the system at low and high mass-damping ratios is different. At high mass-damping ratio, the experimental results indicate that in low reduced velocities the system follow Strouhal law. The power spectrum of the system at this mass ratio and for $\lambda=0.1$ [2] and in $U_r=4.5$ is provided in Fig. 3 (a). As seen, the power spectrum has broad band components and illustrates the deviation of the system from harmonic and periodic behavior. Therefore, the system is out of lock-in range, that is consistent with the experimental results. The Feng's[8] experimental data, shows that at higher reduced velocities, from $U_r=5$ to $U_r=6.5$, the system deviates from the Strouhal law and oscillates at a fixed frequency of $\omega=1$, where ω is the ratio of the frequency of the structural oscillations the vortex-shedding frequency. Therefore the behavior of the system is periodic. The power spectrum of the system, at this range, is depicted in Fig. 3 (b) to 3 (e). As can be seen, the spectral analysis not only predicts the periodic behavior for the system, but also in Fig. 3 (b), at the beginning of the lock-in region, predicts one of its harmonics at the frequency of 0.156, corresponding to $\omega=1$ and shows a big peak at

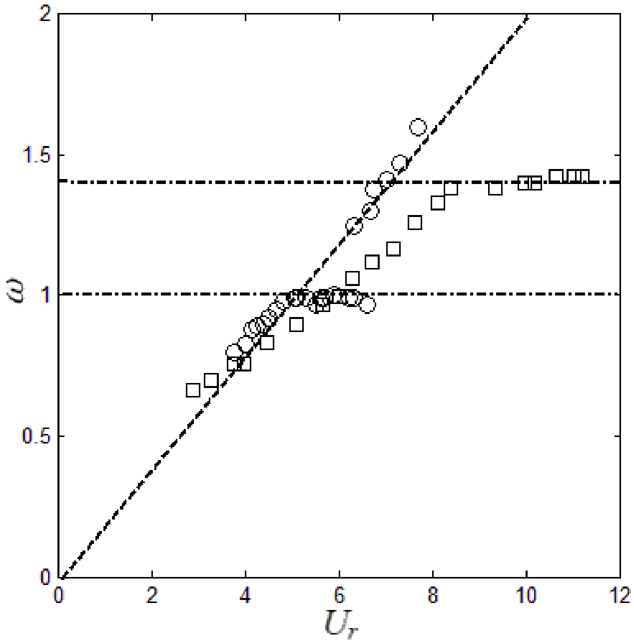

Figure 2. The experimental frequency response. ○, Feng's[8] experimental results at high mass-damping ratio $\mu=194.55$ and $\lambda=0.1$; □, experimental results of Branković and Bearman[9] at low mass-damping ratio; ---, the Strouhal law; -.-, the lock-in frequency.

there. The Fig. 3 (d) shows a spectrum with broad band components. It suggests that in the lock-in domain, From $U_r=5$ to $U_r=6.5$, in a short range of reduced velocity the system will oscillate out of lock-in manner. Referring to the experimental results of Feng[8] shows that in this range of reduced

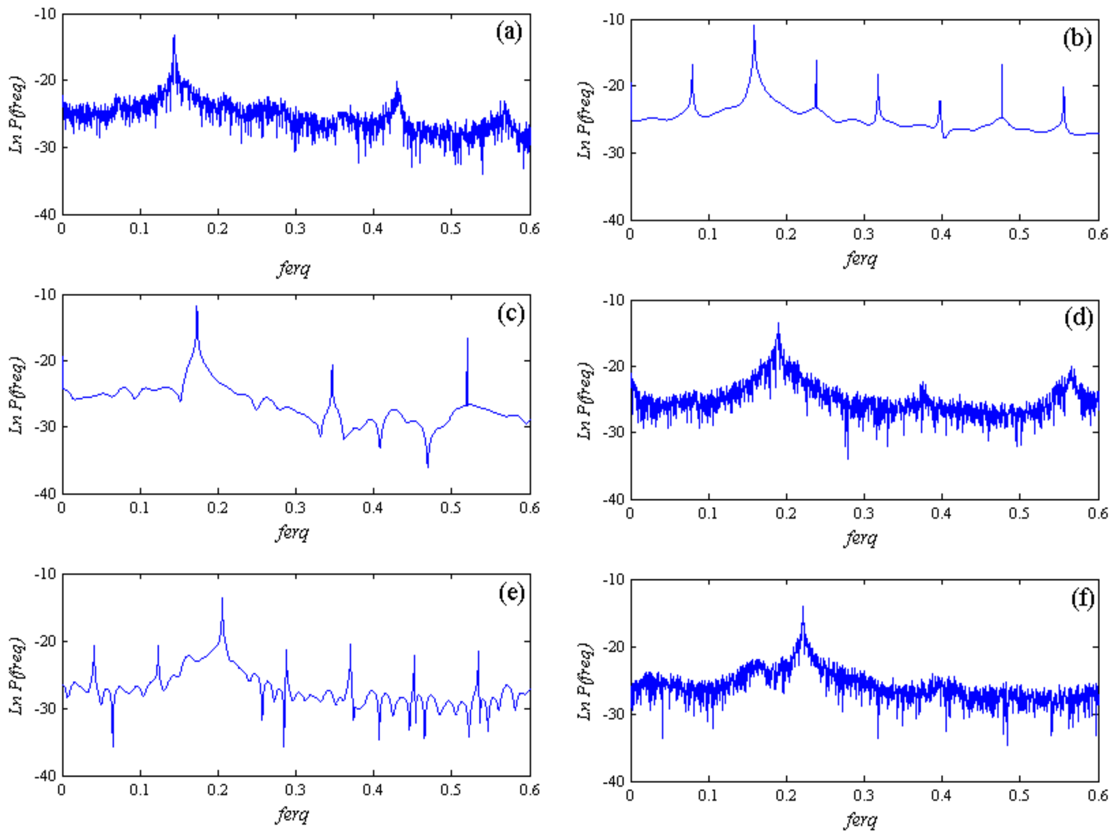

Figure 3. The power spectrum of the system corresponding to Feng's experimental data. (a) $U_r=4.5$; (b) $U_r=55$; (c) $U_r=5.5$; (d) $U_r=6$; (e) $U_r=6.5$; (f) $U_r=7$.

velocity the system have leaved the lock-in domain and followed the Strouhal law. Fig. 3 (f) shows the power spectrum of the system at $U_r=7$, where the system have leaved the lock-in domain and follows the Strouhal law again. As it is expected the spectrum has broad band components.

Fig. 2 also shows the experimental results of Branković and Bearman[9] that was conducted at low mass-damping ratio. According to this experimental results, it is expected that first the power spectrum of the system has broad band components. Then when the system undergoes the lock-in phenomenon, the power spectrum predicts periodic behavior for the system. Finally, when the system leaves the lock-in range, the power spectrum will have broad band components again. Fig. 4 shows the power spectrum at $\mu=1.1615$ and $\xi=1.5\times10^{4}$, corresponding to these experimental results. It illustrates that the spectral analysis not only predicts the lock-in domain precisely, but also accurately predicts the lock-in frequency and the change of the behavior of the system. For example, Fig 4 (b), at the beginning of the lock-in range, shows a big peak at the frequency of 0.23, corresponding to ω=1.4.

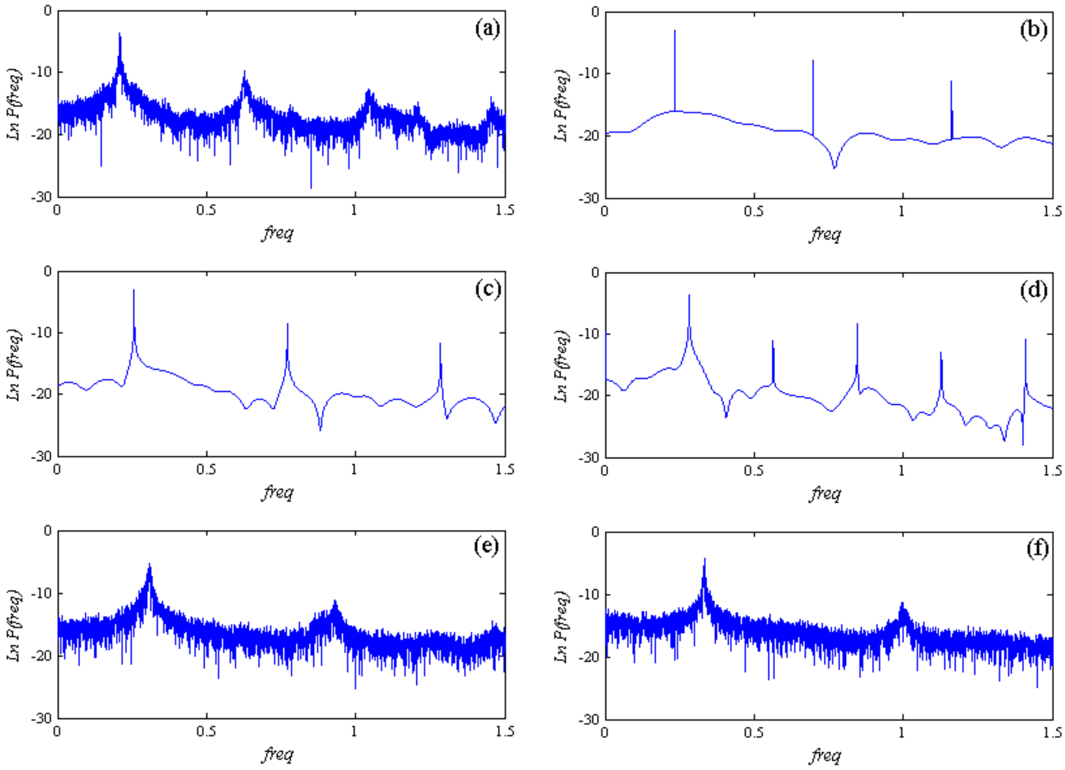

Figure 4. The power spectrum of the system corresponding to Branković and Bearman's[9] experimental data. (a) $U_r=8$; (b) $U_r=9$; (c) $U_r=10$; (d) $U_r=11$; (e) $U_r=12$; (f) $U_r=13$.

Therefore the spectral analysis of the wake oscillator model can be used as a criterion for predicting of the lock-in range in both low and high mass-damping ratios.

4. Verification of the Griffin plot

The maximum structure displacement amplitude at lock-in is expressed as a function of a single combined mass-damping parameter, namely the Skop-Griffin parameter S_G[3],

$$S_G = 8\pi^2 S_t^2 \mu\xi = \frac{C_{L0}\xi}{2M} \tag{6}$$

yielding the so-called Griffin plot . Verifying the validity of the Griffin plot by analytical analysis of wake oscillator model, a reference resonance state is defined as $\omega=1$ and $\Omega=1$[3]. By this definition, Eq. (4) yields

$$\begin{cases} \ddot{y} + \lambda\dot{y} + y = Mq \\ \ddot{q} + \varepsilon(q^2 - 1)\dot{q} + q = A\ddot{y} \end{cases} \tag{7}$$

The appropriate analytical procedure to find the oscillatory solutions of Eq. (7) is the averaging method[6]. For this purpose, let us express q and y in the form

$$q = \mathrm{R}_1\cos(\omega t + \theta_1) \qquad y = R_2\cos(\omega t + \theta_2) \tag{8}$$

Using this method, we can show that the amplitudes R_1 and R_2 and the phase difference $\varphi=\theta_1+\theta_2$ between y and q satisfy the following set of first order differential equations

$$\begin{cases} \dot{R}_1 = \frac{\varepsilon R_1}{2}\left(1 - \frac{R_1^2}{4}\right) - \frac{AR_2}{2}\sin\varphi \\ \dot{R}_2 = -\frac{1}{2}\lambda R_2 - \frac{MR_1}{2}\sin\varphi \\ \dot{\varphi} = -\frac{1}{2}\left(\frac{MR_1}{R_2} + \frac{AR_2}{R_1}\right)\cos\varphi \end{cases} \tag{9}$$

In the stationary state, Eqs. (9) lead to the following solutions depending on the value of the phase difference φ between q and y. With the $\varphi=\pi/2$ and $\varphi=-\pi/2$ the solutions, respectively, are

$$R_1^2 = 4\left(1 + \left(\frac{A}{\varepsilon}\right)\left(\frac{M}{\lambda}\right)\right) \tag{10}$$

$$R_2 = \frac{M}{\lambda}R_1 \tag{11}$$

Substituting Eq. (10) in Eq. (11), yields

$$R_2 = 2\left(\frac{M}{\lambda}\right)\sqrt{1 + \left(\frac{A}{\varepsilon}\right)\left(\frac{M}{\lambda}\right)} \tag{12}$$

The λ/M can be written in the terns of the Skop-Griffin parameter S_G. Using Eqs. (5) and (6) and considering $M=0.05/\mu^3$, then λ/M is obtained as

$$\frac{\lambda}{M} = \frac{4S_G}{C_{L0}} + 20\gamma\Omega \tag{13}$$

Therefore the Eq. (12) shows the maximum amplitude of structure R_1 as a function of S_G, a combined mass-damping parameter. Fig. 5 shows the comparison of the analytical results of the classical wake oscillator model, Eq. (12), with the experimental results of the Griffin plot. It illustrates that the analytical results agree with the trend of the experimental data. But the oscillatory states are not always realized even if from Eqs. (10) and (11) we obtain values for R_1 and R_2. Their realization is physically interesting only so long as they are stable[10]. To study the stability of these fixed points, the linearization method is used. In this method the behavior of the system linearized in the neighborhood of these points, is determined by the eigenvalues of the Jacobian matrix. The Jacobian matrices of the system of the slow-flow equations, at fixed points, are

$$J_{\pm\left(\frac{\pi}{2}\right)} = \begin{pmatrix} \frac{\varepsilon}{2}\left(-2 - 3\left(\frac{A}{\varepsilon}\right)\left(\frac{M}{\lambda}\right)\right) & \mp\frac{A}{2} & 0 \\ \mp\frac{M}{2} & -\frac{\lambda}{2} & 0 \\ 0 & 0 & -\frac{1}{2}\left(\frac{\lambda^2 + AM}{\lambda}\right) \end{pmatrix} \tag{14}$$

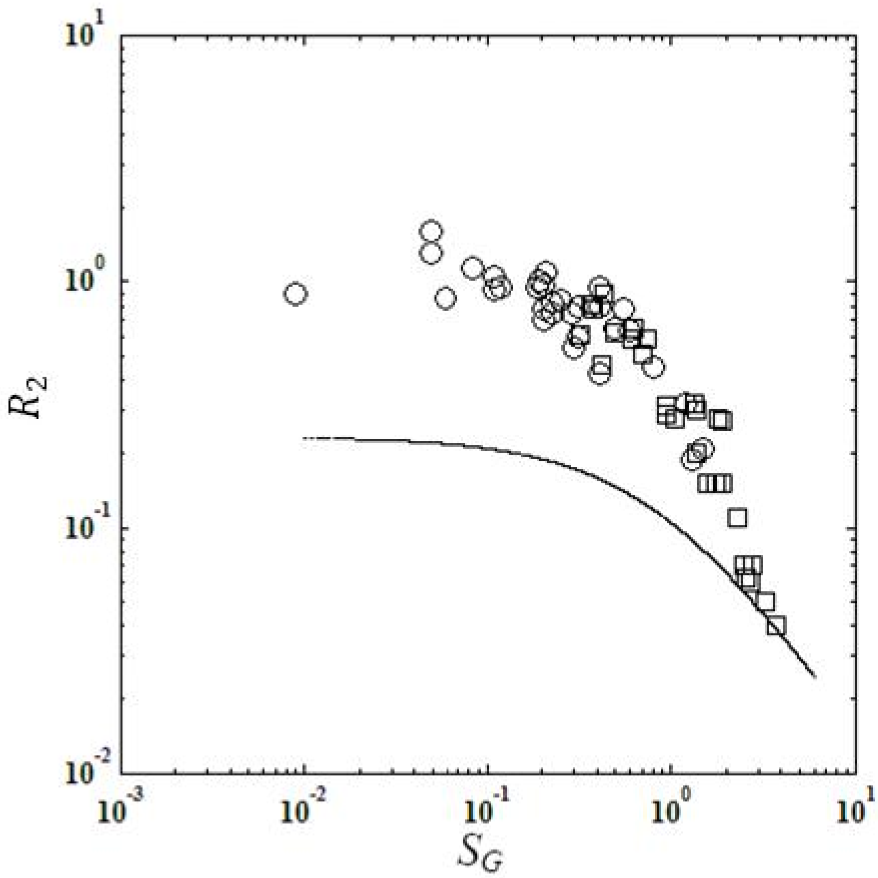

Figure 5. The Griffin plot. –, based on the classical wake oscillator model. Empirical data in water: ○; Empirical data in air: □.

Where $J_{\pi/2}$ and $J_{-\pi/2}$, respectively, are the Jacobian matrices when $\varphi=\pi/2$ and $\varphi=-\pi/2$. Assuming $\lambda=0.1$, Fig. 6 shows the eigenvalues of $J_{\pi/2}$ and $J_{-\pi/2}$ with respect to S_G.

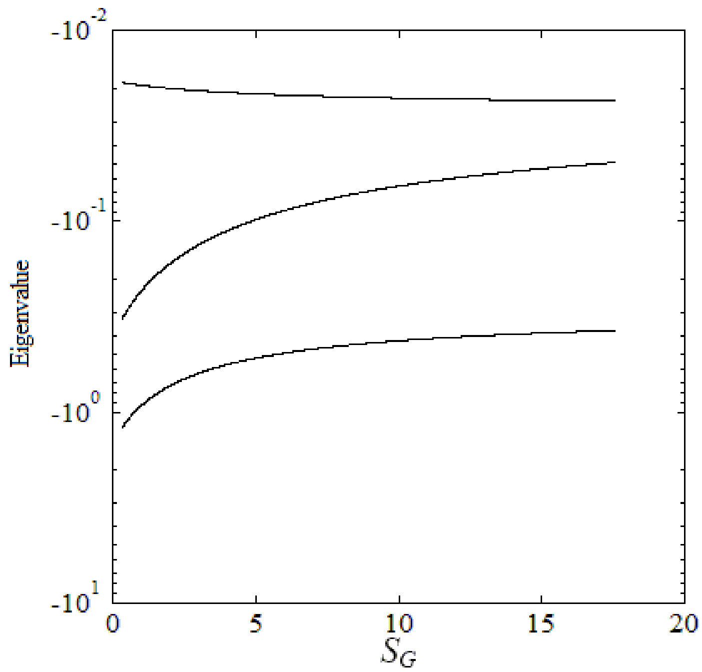

Figure 6. The eigenvalues of $J_{\pi/2}$ and $J_{-\pi/2}$

As seen all eigenvalues are negative, therefore the oscillatory states obtained in Eqs. (10) and (11) are stable. So the results of Eq. (12), which express the maximum amplitude of the structural oscillations as a function of S_G, are valid. Therefore it can be said that a combined mass-damping parameter, S_G, can reasonably collapse peak amplitude in the Griffin plot.

Conclusions

This paper dealt with the lock-in phenomenon as one of important subjects in the dynamics of coupled fluid-structure systems. In the first part of the paper, the spectral analysis of the wake oscillator model was used as a criterion for predicting the lock-in domain. This analysis showed that the spectral analysis predicts a periodic motion at lock-in and gives peak at the frequency in which lock-in occurs. Non-synchronized dynamics of the coupled system, gives broad band components to the spectrum. Despite of the different behaviors of the system in low and high mass ratios, the results of the spectral analysis, in both high and low mass ratios, was quite consistent with the experimental results.

In the next section, the validity of the Griffin plot was analytically investigated. First, using an averaging method, the slow-flow equations of the system were derived. Then, their solutions in the stationary state, were obtained. To show that these solutions are physically interesting, their stability was analyzed. These analytical investigations showed that a combined mass-damping parameter can reasonably collapse peak amplitude data in the Griffin plot.

These numerical and analytical investigations, respectively, can be used for practically predicting of lock-in range and verification of extensive use of the Griffin plot by practical engineers.

REFERENCES

1 R.D. Blevins, *Flow-Induced Vibrations*, Van Nostrand Reinhold, New York, 1990.

2 E. de Langre, Frequency lock-in is caused by coupled-mode flutter, *Journal of Fluids and Structures*, 2006, **22**, 783-791.

3 M.L. Facchinetti, E. de Langre, F. Biolley, Coupling of structure and wake oscillators in vortex-induced vibrations, *Journal of Fluids and Structures*, 2004, **19**, 123–140.

4 A. Khalak, C.H.K. Williamson, Motions, forces and mode transitions in vortex-induced vibrations at low mass-damping, *Journal of Fluids and Structures*, 1999, **13**, 813-851.

5 C.H.K. Williamson, R. Govardhan, Vortex-induced vibrations, *Annual review of fluid mechanics*, 2004, **36**, 413-455.

6 A.H. Nayfeh, *Introduction to Perturbation Techniques*, Wiley, New York, 1993.

7 M.S. Pantazopoulos, Vortex-induced vibration parameters: critical review, *Proceedings the 17th International Conference on Offshore Mechanics and Arctic Engineering*, 1994, Osaka, Japan, 199−255.

8 C.C. Feng, *The measurement of vortex-induced effects in flow past a stationary and oscillating circular and D-section cylinders*. Master's Thesis, University of British Columbia, Vancouver.

9 M. Branković, P.W. Bearman, Measurements of transverse forces on circular cylinders undergoing vortex-induced vibration, *Journal of Fluids and Structures*, 2006, **22**, 829–836.

10 P. Woafo, Harmonic oscillations, chaos and synchronization in systems consisting of van der Pol oscillator coupled to a linear oscillatr, *The Abdus Salarn International Centre for Theoretical Physics*, 1999, IC/188.